



UNIVERSITY
OF WOLLONGONG
AUSTRALIA

University of Wollongong
Research Online

Faculty of Engineering - Papers (Archive)

Faculty of Engineering and Information Sciences

2010

Mechanical Model of a Floating Oscillating Water Column Wave Energy Conversion Device

Brad Stappenbelt

University of Wollongong, brads@uow.edu.au

Paul Cooper

University of Wollongong, pcooper@uow.edu.au

<http://ro.uow.edu.au/engpapers/551>

Publication Details

Stappenbelt, B. & Cooper, P. (2010). Mechanical Model of a Floating Oscillating Water Column Wave Energy Conversion Device. 2009 Annual Bulletin of the Australian Institute of High Energetic Materials, 1 34-45.

Research Online is the open access institutional repository for the University of Wollongong. For further information contact the UOW Library:
research-pubs@uow.edu.au

Mechanical model of a floating oscillating water column wave energy conversion device

Stappenbelt B.^{*}, Cooper P.

School of Mechanical, Materials and Mechatronic Engineering, University of Wollongong, Australia

Abstract:

The study of floating oscillating water column (OWC) wave energy conversion (WEC) device performance includes analysis of the dynamic coupling of the water column and the floating structure. In the present investigation, a mechanical oscillator model was proposed in order to examine this relationship for the heave motion of a floating wave energy conversion device. Characterisation of the dynamic system optimal behaviour was performed by examining the effect of relative OWC and floating structure natural frequencies, the phase relationships of the various system components and the optimal power take-off damping of the system. It was determined that separation of the natural frequencies results in significant increases in maximum power capture. When the OWC and structure natural frequencies are coincident the motions are essentially in phase and limited power capture is achieved. For optimal power capture the separation of the natural frequencies should be such that the floating structure has the lower natural frequency. This should also generally result in improved alignment of the system resonant response with the available wave power. The model also provides evidence of the capacity of power take-off damping control to improve the non-resonant performance of the OWC WEC device in a spectrally distributed wave environment.

Keywords: oscillating water column, wave energy converter, power take-off, floating structure, power capture

1. INTRODUCTION

Oscillating water column (OWC) wave energy conversion devices consist of a partially submerged chamber open to wave forces at the base as illustrated in Figure 1. The wave forces cause the water column within the chamber to rise and fall, driving the air in and out (inhalation and exhalation) of the chamber typically through a Wells or variable pitch type air turbine. An electrical generator is then utilised to convert the oscillatory airflow established into electrical energy. The pneumatic gearing provided by the air coupling facilitates the conversion of low frequency wave power into high frequency electrical power.

Oscillating water column type wave energy conversion devices can be located near-shore as a fixed structure or offshore in a floating moored-structure configuration. Much analytical, numerical and experimental work has been undertaken on fixed (e.g. Morris-Thomas & Irvin, 2007) and floating (e.g. Chudley, Mrina, Ming & Johnson (2002)) oscillating water column wave energy conversion. A number of concepts have been demonstrated at scale prototype including the Limpet (Boake, Whittaker, Folley & Ellen 2002), Oceanlinx's near-shore OWC (Gray, 2007) and the Pico plant (Brito-Melo, Neuman & Sarmiento, 2008).

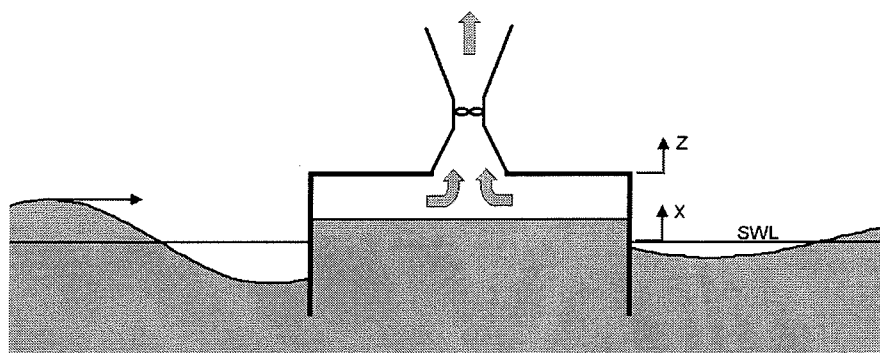


Figure 1 Floating Oscillating Water Column Wave energy device (air flow arrows indicate the exhalation phase).

The analysis of floating oscillating water column wave energy conversion devices involves the coupled

dynamics of the water column and the floating structure. Mechanical oscillator models have seen

considerable use in the study of wave energy converters including oscillating water column wave energy devices (Folley & Whittaker, 2005; Falnes & McIver, 1985; Thiruvenkatasamy, Neelamani & Sato, 1998). This simplified approach, which does not analyse the full hydrodynamic complexity of the situation, provides clear indication of device performance trends and is particularly useful in the preliminary design and model testing development phases. It can provide a more general description of the system behaviour compared to complex numerical approaches, allowing for greater ease in determining optimal performance.

Adoption of mechanical oscillator modelling to fixed OWC WEC devices for example has provided valuable information regarding optimal power capture and power take-off damping conditions (Mei, 1976). The optimum operating state for a fixed OWC is, predictably, the condition where the oscillating water column natural frequency (dependent primarily on the effective length of the water column) is set at the incident wave frequency. Under this resonant condition, the optimum power take-off damping is theoretically equal to the OWC radiation damping (*i.e.* $\lambda=b$). In practice, when resonant conditions cannot be attained (or the wave energy is spread across a range of frequencies), a larger power take-off damping is optimal to broaden the region over which significant power capture is achieved.

The aim of the present study was to analytically investigate the maximum power capture of a floating oscillating water column wave energy conversion device in heave by introducing a floating system mechanical oscillator model. The focus of the investigation was the influence of relative OWC and floating structure natural frequencies on maximum power capture and the corresponding optimal power take-off damping. The phase of the OWC and the floating structure were also examined.

2. WAVE ENERGY CONVERTER MODEL

The basis of the floating OWC heave motion mechanical oscillator model utilised in the present study (Figure 2) was the fixed OWC model proposed by Szumko (1989) and more recently adopted by Folley & Whittaker (2005) with the inclusion of air compressibility. The lower-case variables k , b and m are the OWC water plane stiffness, radiation damping and mass respectively. The corresponding upper-case parameters for the floating structure are K , B and M . The mass terms include the hydrodynamic mass. It must be noted that for the floating structure, K also includes the mooring line stiffness. The turbine damping is modelled by the linear damping parameter λ and the air compressibility by the linear stiffness μ . The x coordinate is the OWC mean free surface elevation and z is the floating structure displacement relative to the still-water level (see also Figure 1).

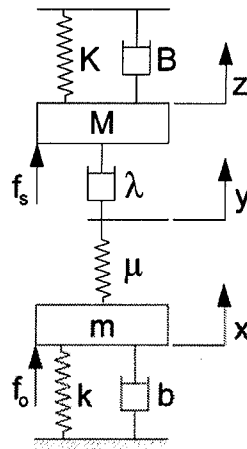


Figure 2 Discrete mass-spring-damper model of the heave motions of a floating OWC WEC device

The equations of motion of the system illustrated in Figure 2 are

$$m \frac{d^2 x}{dt^2} + b \frac{dx}{dt} + kx + \mu(x - y) = f_o \quad (1)$$

$$\lambda \frac{d(y - z)}{dt} + \mu(y - x) = 0 \quad (2)$$

$$M \frac{d^2 z}{dt^2} + B \frac{dz}{dt} + \lambda \frac{d(z - y)}{dt} + Kz = f_s \quad (3)$$

The wave forces on the OWC, f_o , and the floating structure, f_s , are assumed to be related via the parameter r (see Eq. 4). In general r is complex, allowing for both a magnitude and phase difference between the forces. In the present analysis, the

floating OWC is assumed to be axisymmetric. For linear waves, using the Froude-Krylov assumption as a first estimate of the wave induced heave force, it may be shown that the parameter r is therefore real. In the limit of large wavelength, or small wave number, r can also be shown to be equivalent to the area ratio of the OWC opening to the total base area of the floating wave energy converter.

$$\left. \begin{aligned} f_o &= rf \\ f_s &= (1-r)f \end{aligned} \right\} 0 \leq r \leq 1 \quad (4)$$

The complex representation of the harmonic solution of the equations of motion of the system is

$$f = Fe^{i\omega t} \quad x = Xe^{i\omega t} \quad y = Ye^{i\omega t} \quad z = Ze^{i\omega t} \quad (5)$$

Eqs. 1-3 then become

$$(k + \mu - m\omega^2 + i b\omega)X - \mu Y = Fr \quad (6)$$

$$\mu X - (\mu + i\lambda\omega)Y + i\lambda\omega Z = 0 \quad (7)$$

$$(K - M\omega^2 + i\omega(B + \lambda))Z - i\lambda\omega Y = F(1-r) \quad (8)$$

Making the substitutions $\alpha = k - m\omega^2$, $\beta = b\omega$, $\gamma = K - M\omega^2$, $\delta = B\omega$ and $\Lambda = \lambda\omega$ and solving the set of simultaneous equations (Eqs. 6-8) yields

$$X = \frac{Fr(\gamma + i\delta)\Lambda + F(\Lambda + r(\delta - i\gamma))\mu}{(\alpha + i\beta)(\gamma + i\delta)\Lambda + ((\gamma + i\delta)\Lambda + \alpha(\delta + \Lambda - i\gamma) + \beta(\gamma + i(\delta + \Lambda)))\mu} \quad (9)$$

$$Y = \frac{F(1-r)(\alpha + i\beta)\Lambda + F(\Lambda + r(\delta - i\gamma))\mu}{(\alpha + i\beta)(\gamma + i\delta)\Lambda + ((\gamma + i\delta)\Lambda + \alpha(\delta + \Lambda - i\gamma) + \beta(\gamma + i(\delta + \Lambda)))\mu} \quad (10)$$

$$Z = \frac{F(1-r)(\alpha + i\beta)\Lambda + F((1-r)\beta + \Lambda - i(1-r)\alpha)\mu}{(\alpha + i\beta)(\gamma + i\delta)\Lambda + ((\gamma + i\delta)\Lambda + \alpha(\delta + \Lambda - i\gamma) + \beta(\gamma + i(\delta + \Lambda)))\mu} \quad (11)$$

Substituting the solutions for Z and Y into the OWC power capture relationship

$$P = \frac{\Lambda\omega|Z - Y|^2}{2} \quad (12)$$

results in Eq. 13 for the power capture, P .

$$P = \frac{\Lambda\omega\mu^2|F|^2 \left((1-r)^2(\alpha^2 + \beta^2) - 2r(1-r)(\alpha\gamma + \beta\delta) + r^2(\gamma^2 + \delta^2) \right)}{2(\alpha^2 + \beta^2)(\gamma^2 + \delta^2)\Lambda^2 + 4(\gamma(\beta^2 + \alpha(\alpha + \gamma)) + \alpha\delta^2)\Lambda^2\mu + 2((\alpha^2 + \beta^2)(\gamma^2 + \delta^2) + 2(\alpha^2\delta + \beta(\gamma^2 + \delta(\beta + \delta)))\Lambda + ((\alpha + \gamma)^2 + (\beta + \delta)^2)\Lambda^2)\mu^2} \quad (13)$$

The optimal damping may then be determined by setting the partial derivative of the power capture with respect to

the power take-off damping equal to zero (i.e. $\partial P / \partial \Lambda = 0$), yielding

$$\Lambda_{opt}^2 = \frac{(\alpha^2 + \beta^2)(\gamma^2 + \delta^2)\mu^2}{(\alpha^2 + \beta^2)(\gamma^2 + \delta^2) + 2(\gamma(\beta^2 + \alpha(\alpha + \gamma)) + \alpha\delta^2)\mu + ((\alpha + \gamma)^2 + (\beta + \delta)^2)\mu^2} \quad (14)$$

Interestingly, the optimal damping is independent of the wave force, F , and the force ratio, r . The maximum power capture for the OWC, is then obtained by

substituting the optimal damping into Eq. 13, resulting in the expression

$$P_{max} = \frac{|F|^2 \left((1-r)^2(\alpha^2 + \beta^2) - 2r(1-r)(\alpha\gamma + \beta\delta) + r^2(\gamma^2 + \delta^2) \right) \sqrt{(\alpha^2 + \beta^2)(\gamma^2 + \delta^2)\mu^2\omega}}{4(\alpha^2 + \beta^2)(\gamma^2 + \delta^2) \sqrt{(\alpha^2 + \beta^2)(\gamma^2 + \delta^2) + 2(\gamma(\beta^2 + \alpha(\alpha + \gamma)) + \alpha\delta^2)\mu + ((\alpha + \gamma)^2 + (\beta + \delta)^2)\mu^2} + 4(\alpha^2\delta + \beta(\gamma^2 + \delta(\beta + \delta))) \sqrt{(\alpha^2 + \beta^2)(\gamma^2 + \delta^2)\mu^2}} \quad (15)$$

Defining the ratios $Q = \frac{\alpha}{\beta}$, $R = \frac{\alpha}{\mu}$, $S = \frac{\gamma}{\delta}$ and $T = \frac{\gamma}{\mu}$,

for mathematical convenience, the optimal damping and maximum power capture may be expressed as

$$\Lambda_{opt}^2 = \frac{(1+Q^2)R^2(1+S^2)T^2\mu^2}{Q^2(1+S^2)T^2 + 2QRT(S+QT+QS^2(1+T)) + (1+Q^2)R^2(T^2+S^2(1+T)^2)} \quad (16)$$

and

$$P_{max} = \frac{|F|^2 \sqrt{(1+Q^2)R^2(1+S^2)T^2} \left((1+Q^2)(1-r)^2 R^2 S^2 - 2r(1-r)QRS(1+QS)T + Q^2 r^2 (1+S^2)T^2 \right) \omega}{4RT\mu \left((1+Q^2)R(1+S^2)T \sqrt{Q^2(1+S^2)T^2 + 2QRT(S+QT+QS^2(1+T)) + (1+Q^2)R^2(T^2+S^2(1+T)^2)} + \sqrt{(1+Q^2)R^2(1+S^2)T^2} \left((1+Q^2)RS + Q(1+S^2)T \right) \right)} \quad (17)$$

The parameters Q and R are respectively the tuning and air-compliance parameters adopted by Folley & Whittaker (2005).

The optimal damping at the OWC and floating structure natural frequencies may then be shown to be

$$\lambda_{opt}^2 = \frac{b^2 m (B^2 k m + (K m - k M)^2) \mu^2}{2 b B k m^2 \mu^2 + m (B^2 k m + (K m - k M)^2) \mu^2 + b^2 k (B^2 k m + (k M - m (K + \mu))^2)} \quad \text{and} \quad (18)$$

$$\lambda_{opt}^2 = \frac{B^2 M (K^2 m^2 + K (b^2 - 2 k m) M + k^2 M^2) \mu^2}{2 b B K M^2 \mu^2 + M (K^2 m^2 + K (b^2 - 2 k m) M + k^2 M^2) \mu^2 + B^2 K (K^2 m^2 + M^2 (k + \mu)^2 + K M (b^2 - 2 m (k + \mu)))} \quad \text{respectively.} \quad (19)$$

1. Fixed OWC WEC Device

The fixed OWC solution (Folley & Whittaker, 2005) can be retrieved by setting $S \rightarrow \infty$ and $T \rightarrow \infty$ (i.e. $K \rightarrow \infty$);

$$\Lambda_{opt_f}^2 = \frac{(1 + Q^2) R^2 \mu^2}{R^2 + Q^2 (1 + R)^2} \quad \text{and} \quad (20)$$

$$P_{max_f} = \frac{|Fr|^2 Q^2 \omega}{4 \mu (QR + \sqrt{R^2 + Q^2 (1 + R)^2} \sqrt{(1 + Q^2) R^2})} \quad (21)$$

The forcing term Fr is the force on the oscillating water column. The limiting case of incompressible air for a fixed OWC may be obtained by setting $R \rightarrow 0$ (i.e. $\mu \rightarrow \infty$)

$$P_{max_f_incomp} = \frac{|Fr|^2}{4 b (1 + \sqrt{(1 + Q^2)})} \quad (22)$$

The ratio of maximum fixed OWC power capture ratio for the compressible and incompressible flow cases is then

$$\frac{P_{max_f}}{P_{max_f_incomp}} = \frac{QR (1 + \sqrt{1 + Q^2})}{QR + \sqrt{R^2 + Q^2 (1 + R)^2} \sqrt{(1 + Q^2) R^2}} \quad (23)$$

In interpreting Eq. 23, the relationship between the expressions for Q and R , stated previously, must be considered. Solving these equations yields

$$Q = \frac{\mu}{\beta} R = \frac{\mu}{b \omega} R \quad (24)$$

This implies that for any real system of interest (i.e. positive OWC radiation damping and positive air compliance) only the first and third quadrants of the plot are possible solutions. Plotting these quadrants from the ratio of maximum fixed OWC power capture ratio for the

compressible and incompressible flow expression (Eq. 23)

in Figure 3 replicates the result reported by Folley & Whittaker (2005).

In the development of the Folley and Whittaker model, it was mathematically convenient to represent the system in terms of tuning and compressibility parameters. Physical interpretation of the data in this form is difficult however for two reasons; firstly, the parameters have complex physical meaning and more importantly, the parameters are inter-related. It is useful therefore to recast the power capture equation in terms of the wave or excitation frequency. The parameters Q and R may be represented as a function of the ratio of the wave frequency to the incompressible system natural frequency, Ω_o , as

$$\left. \begin{aligned} Q &= \frac{\alpha}{\beta} = \frac{k - m \omega^2}{b \omega} = \frac{1}{2 \zeta_o} \left(\frac{1}{\Omega_o} - \Omega_o \right) \\ R &= \frac{\alpha}{\mu} = \frac{k - m \omega^2}{\mu} = \kappa_o (1 - \Omega_o^2) \end{aligned} \right\} \quad (25)$$

Three new parameters (Eqs. 26–28) are introduced. Eq. 26 is the ratio of the radiation damping to the critical damping of the system without the turbine (i.e. $\lambda \rightarrow 0$). Eq. 27 is the ratio of water plane stiffness to air compressibility spring rate and Eq. 28 is the ratio of the excitation frequency to the undamped natural frequency.

$$\zeta_o = \frac{b}{2 \sqrt{k m}} = \frac{b}{c_{cr}} \quad (26)$$

$$\kappa_o = \frac{k}{\mu} \quad (27)$$

$$\Omega_o = \frac{\omega}{\omega_{no}} \quad (28)$$

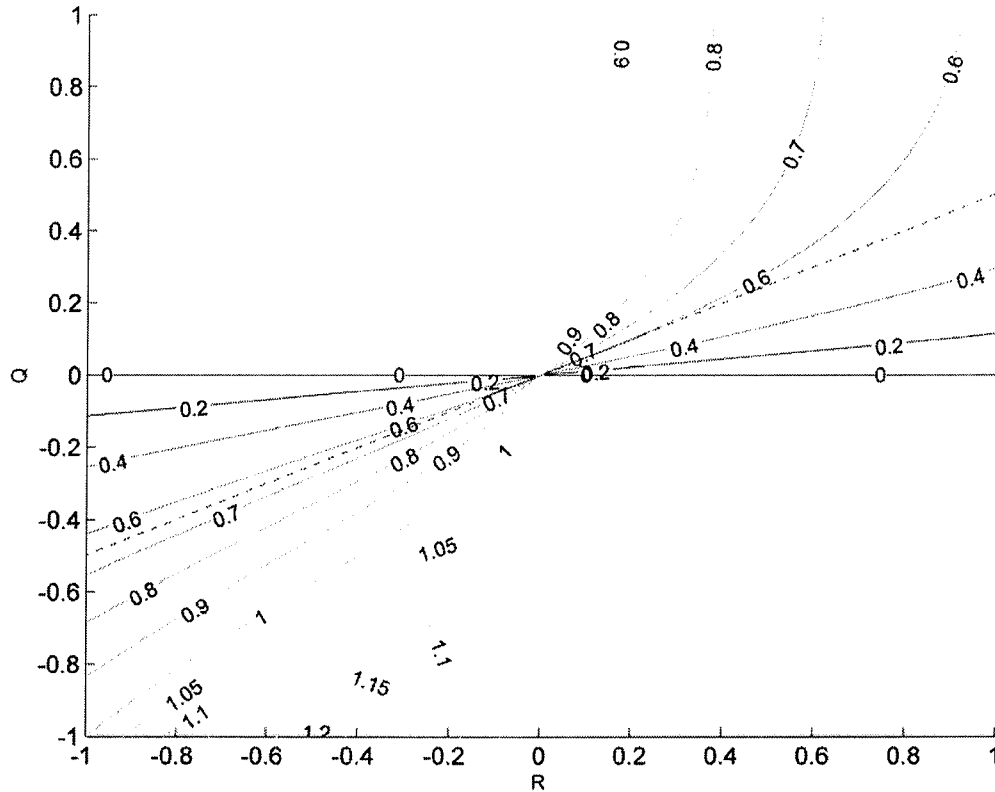


Figure 3 - Maximum fixed OWC power capture ratio for compressible and incompressible flow; the dashed line represents the frequency response for the case $\kappa_0=100$, $\zeta_0=0.01$.

These commonly employed and readily physically interpretable parameters then define the frequency response for the system as expressed in Eq. 29 and

plotted (as the dashed line for a particular case) in Figure 3.

$$\frac{P_{\max_f}}{P_{\max_f_incomp}} = \frac{\kappa_0 (\Omega_0^2 - 1)^2 \left(2\zeta_0 + \sqrt{4\zeta_0^2 - 2 + \Omega_0^2 + \frac{1}{\Omega_0^2}} \right)}{2\zeta_0 \kappa_0 (\Omega_0^2 - 1)^2 + \Omega_0 \sqrt{\left(4\zeta_0^2 - 2 + \Omega_0^2 + \frac{1}{\Omega_0^2} \right) \left(\kappa_0 - \kappa_0 \Omega_0^2 \right)^2} \sqrt{4\zeta_0^2 \kappa_0^2 (\Omega_0^2 - 1)^2 + \left(\Omega_0^2 - 2 + \frac{1}{\Omega_0^2} \right) (1 + \kappa_0 - \kappa_0 \Omega_0^2)^2}} \quad (29)$$

2. Floating OWC WEC Device

The floating OWC maximum power capture can be normalised to yield the following expression

$$\hat{P} = \frac{P_{\max}}{(|F|^2 \omega_n / \mu)} = \frac{\sqrt{(1+Q^2)R^2(1+S^2)T^2} \left((1+Q^2)(1-r)^2 R^2 S^2 - 2r(1-r)QRS(1+QS)T + Q^2 r^2 (1+S^2)T^2 \right) \Omega_0}{4RT \left((1+Q^2)R(1+S^2)T \sqrt{Q^2(1+S^2)T^2 + 2QRT(S+QT+QS^2(1+T))} + (1+Q^2)R^2(T^2+S^2(1+T^2)) + \sqrt{(1+Q^2)R^2(1+S^2)T^2} \left((1+Q^2)RS + Q(1+S^2)T \right) \right)} \quad (30)$$

It can be seen that the frequency response for the floating OWC system is then defined (within the bounds of the parameter space defined by Eq. 30) by both the relationship of Eq. 24 and the expressions

$$S = \frac{1}{2\zeta_s} \left(\frac{1}{\Omega_s} - \Omega_s \right) \quad (31)$$

$$T = \kappa_s (1 - \Omega_s^2)$$

The interpretation of the expression for the maximum power capture of a floating OWC WEC (Eq. 30) is similar to that for the fixed OWC WEC device, except that the solution for a specific case is now represented by a line through four dimensional parameter space. The parameter ζ_s in Eq. 31 is the ratio of the radiation damping to the critical damping of the floating structure without the turbine (i.e. $\lambda \rightarrow 0$). The ratio of water plane stiffness to air compressibility spring rate for the floating structure is denoted κ_s , and the ratio of the excitation frequency to the undamped natural frequency of the floating structure, again without turbine damping, by Ω_s .

3. RESULTS AND DISCUSSION

The water plane stiffness and mass of the OWC and the structure may be related via the relative areas in the horizontal plane. Ignoring the mooring system forces and assuming constant floating OWC cross-section,

$$\frac{K}{k} = \frac{A_s}{A_o} \quad (32)$$

Archimedes principle also dictates that

$$\frac{M}{m} = \frac{\rho l A_s}{\rho l A_o} = \frac{A_s}{A_o} \quad (33)$$

where l is the draft of the structure and ρ is the density of the seawater.

Eqs. 32 and 33 imply that for a uniform cross section device, the OWC and floating structure natural frequencies are equal when mooring forces and added mass are ignored. The present investigation of the effect of relative natural frequency on OWC performance therefore naturally centres on the condition of coincident natural frequencies. In practice, the relative natural frequencies of the system may readily be varied through for example changes in the vertical mooring line stiffness and the geometry of the structure.

The air compressibility spring rate expression may be estimated assuming isentropic compression with only small changes in volume (relative to the total chamber volume). It is expressed in terms of the ratio of specific heats of air, c_p/c_v , atmospheric pressure, p , the OWC water surface area, A , and the chamber height, h , as

$$\mu = \frac{\left(\frac{c_p}{c_v}\right) p A}{h} \quad (34)$$

In conjunction with the water-plane stiffness, $k = \rho g A$, it may be shown that for a practical OWC size (i.e. an effective chamber height of between about 1.5m and 14m), κ_o , the ratio of OWC water-plane stiffness to the air compressibility spring rate, is of the order of 0.1. This means, with a force ratio $r=0.9$, κ_s should be approximately of the order of 0.01.

Figures 4 and 5 present the normalised maximum power capture for a device with a ratio of OWC natural frequency to floating structure natural frequency, Ω_{oss} , of 0.8 and 1.2 respectively. To account for the variation in relative water plane areas, the ratio κ_o/κ_s is scaled as $r/(1-r)$ in these plots. The power capture in all figures presented is normalised as

$$\hat{P} = \frac{P_{max}}{(|F|^2 \omega_{no} / \mu)} \quad (35)$$

The peaks corresponding to the OWC and floating structure natural frequencies are visible in the power capture plots. This is consistent with the floating OWC experimental results from the study by Sykes, Lewis & Thomas (2009). A third, non resonant, peak however is also visible. This is a consequence of a corresponding peak in the optimal power take-off damping at this frequency and is discussed later. Practicalities related to air flow rates through the turbine dictate that $r \rightarrow 1$ is desirable. This directly relates to maximising the OWC area relative to the structure base. From Figures 4 and 5, this implies that a structural natural frequency lower than the OWC natural frequency is favourable in optimising power capture.

At excitation frequencies not coincident with the natural frequencies, optimal damping increases to broaden the region over which significant power capture is achieved. This increase, producing a local maximum in the optimal turbine damping plot (see Figure 7 for example), results in a third peak in the maximum power capture curve between the two natural frequencies. With constant (non-optimal) damping only two peaks corresponding to the system natural frequencies are discernible. This result is in agreement with the experimental and numerical work of Sykes, Lewis & Thomas (2009).

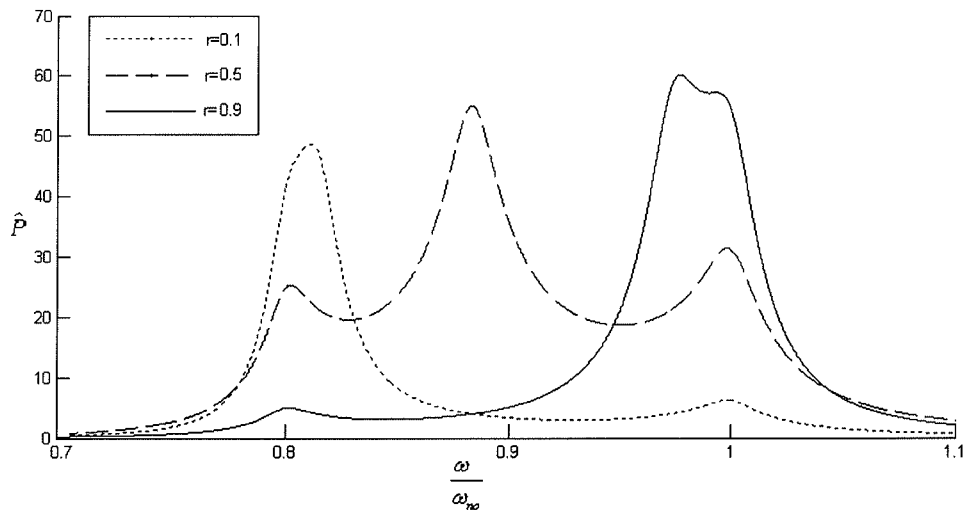


Figure 4 Floating OWC maximum normalised power capture; $\Omega_{os}=0.8$, $\zeta_s=0.01$, $\zeta_o=0.01$, $\kappa_s=0.1$ and $\kappa_o=0.1$ at $r=0$ and $r=1$ respectively.

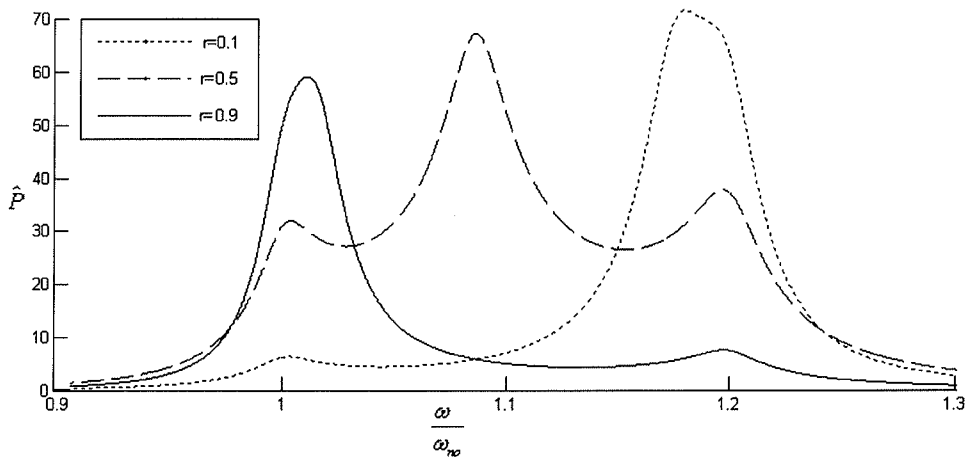


Figure 5 Floating OWC maximum normalised power capture; $\Omega_{os}=1.2$, $\zeta_s=0.01$, $\zeta_o=0.01$, $\kappa_s=0.1$ and $\kappa_o=0.1$ at $r=0$ and $r=1$ respectively.

To illustrate the mechanism by which the use of optimal damping facilitates significant non-resonant maximum power capture, the optimal damping plots corresponding to the power capture curves of Figure 4 are provided in Figures 6~8. The dimensionless damping in Figures 6~8 is presented as $\hat{\Lambda} = \Lambda_{opt} / \mu$. It is evident from Figures 6 to 8 that there exist local minima in the optimal power take-off damping for the floating OWC system at both the structure and OWC natural frequencies. Eqs. 18 and 19 provide an expression for this optimal damping at the OWC and floating structure natural frequencies respectively. These values approach, but do not equal the radiation damping of the OWC (as is the case for a fixed OWC device). The optimal power take-off damping is

strongly influenced by other system parameters also. The optimum power take-off damping at the system natural frequencies are local minima as expected from fixed OWC modelling. A larger power-take-off damping is optimal at frequencies not coincident with the natural frequencies as is the case for a fixed OWC WEC device.

In the case of an air turbine power take-off system, the power take-off damping is a function of the relationship between pressure drop and air flow-rate. A practical limitation to achieving optimal damping and the accompanying non-resonant power gains is therefore the operational range of the turbine.

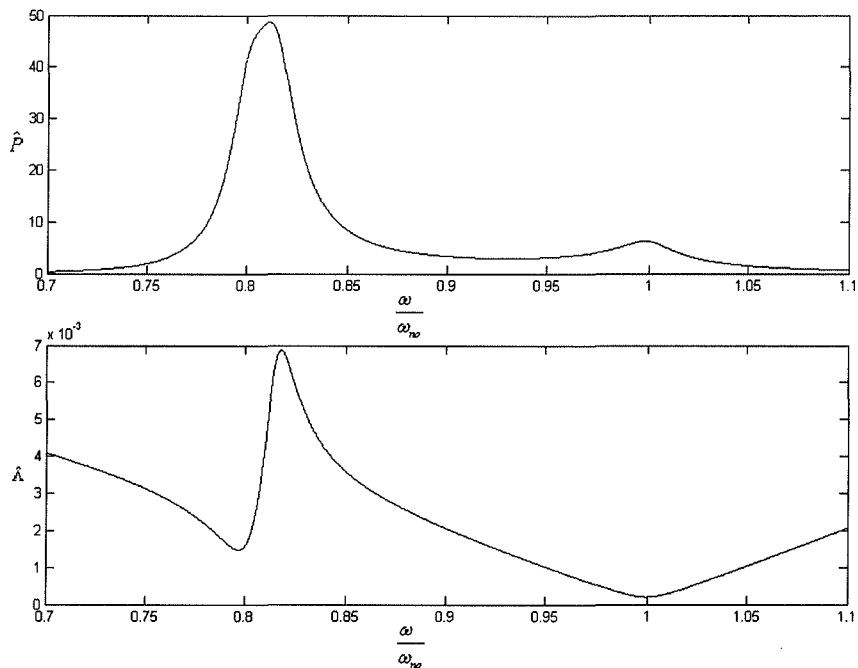


Figure 6 Floating OWC maximum normalised power capture and optimal damping; $\Omega_{os}=0.8$, $r=0.1$, $\zeta_s=0.01$, $\zeta_o=0.01$, $\kappa_s=0.1$ and $\kappa_o=0.1$.

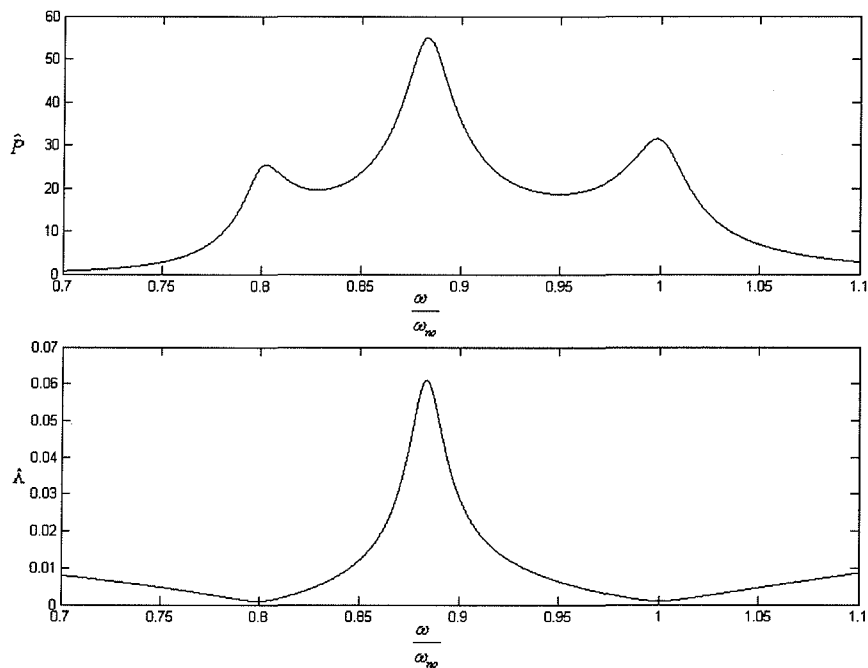


Figure 7 Floating OWC maximum normalised power capture and optimal damping; $\Omega_{os}=0.8$, $r=0.5$, $\zeta_s=0.01$, $\zeta_o=0.01$, $\kappa_s=0.1$ and $\kappa_o=0.1$.

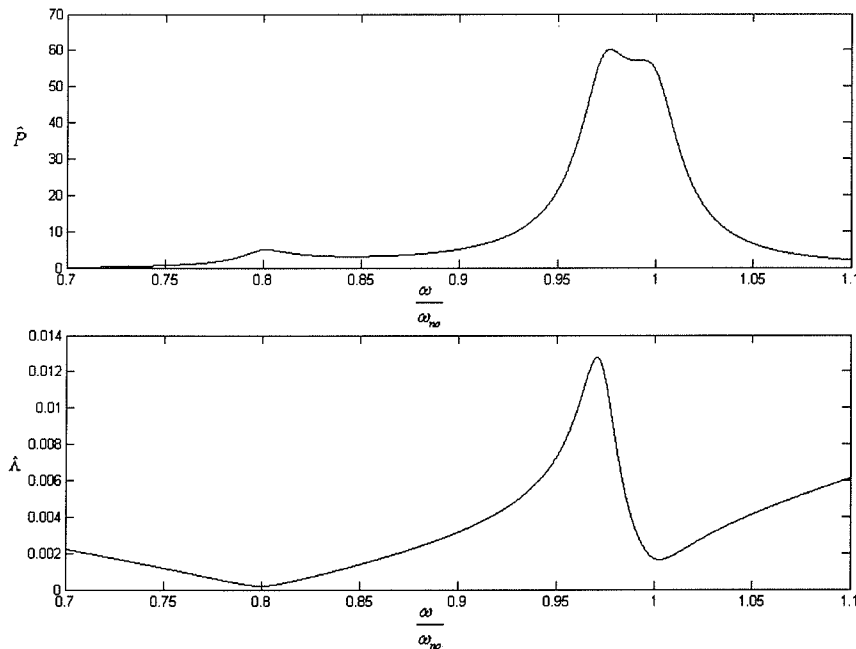


Figure 8 Floating OWC maximum normalised power capture and optimal damping; $\Omega_{os}=0.8$, $r=0.9$, $\zeta_s=0.01$, $\zeta_o=0.01$, $\kappa_s=0.1$ and $\kappa_o=0.1$.

To investigate the effect of oscillating water column and floating structure natural frequency separation, the normalised maximum power is plotted as a function of relative natural frequencies in Figures 9 and 10. A resonant peak corresponding to the OWC natural frequency may be seen at approximately $\omega/\omega_{no}=1$. The floating structure resonant peak is also evident. Since $r=0.9$ in these plots, the power contribution at the

structure natural frequency is significantly less than that at the OWC natural frequency. Evident from these plots is the significant increase in power capture realised when the natural frequencies of the OWC and floating structure are separated. With increasing separation, the maxima in the power capture plots continues to increase.

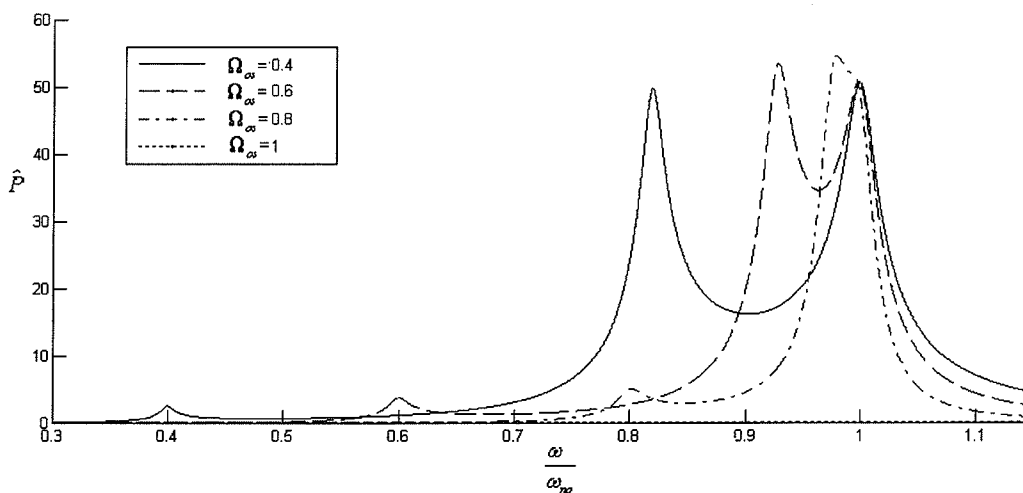


Figure 9 Floating OWC maximum normalised power capture; $r=0.9$, $\zeta_s=0.01$, $\zeta_o=0.01$, $\kappa_s=0.01$, $\kappa_o=0.1$.

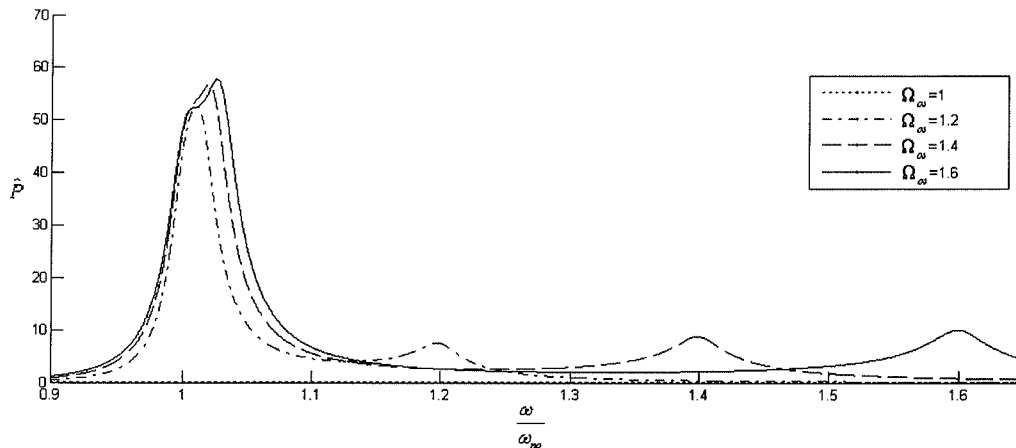


Figure 10 Floating OWC maximum normalised power capture; $r=0.9$, $\zeta_s=0.01$, $\zeta_o=0.01$, $\kappa_s=0.01$, $\kappa_o=0.1$.

For a floating structure, extracting power from the motion of the oscillating water column depends on the relative motion between OWC and structure. The phase difference in these motions is therefore an important consideration in optimising the power capture achieved. The phases of the OWC motion, air motion through the turbine and the floating structure motion, described by the variables X , Y and Z (Eqs. 9-11) respectively were determined by the relationship

$$\phi_x = \arctan \left[\frac{\text{Im}(X/F)}{\text{Re}(X/F)} \right] \quad (36)$$

with similar expressions for ϕ_y and ϕ_z .

The phase plots for two representative cases are presented in Figures 11 and 12. When the natural frequencies coincide (the case $\Omega_{os}=1$ illustrated in Figure 11) the OWC and structure motion are essentially in phase. From Figures 9 and 10 it may be seen that the power capture under this condition is significantly lower. A near 180 degree phase change is observed across the transition through resonance as expected.

When the natural frequencies are separated (illustrated by the case $\Omega_{os}=1.2$ in Figure 12), there are significant phase differences between the motion of the structure and the OWC. This is most evident near the natural frequencies of the structure, resulting in the large maximum power capture in these regions (see Figure 10).

At low κ values (i.e. high air compressibility stiffness relative to the water-plane stiffness) air compressibility effects do not appear to have a significant effect on the phase differences. All cases covered show essentially no phase difference between the air motion through the turbine and the motion of the water column.

4. CONCLUSIONS

Several significant dynamic response characteristics of a floating OWC system were identified. These are potentially useful in the preliminary development phase of a floating OWC WEC device.

Two resonant peaks corresponding to the OWC and structure natural frequencies are evident in the maximum power capture plot. The optimal damping values at these frequencies are local minima as expected from fixed OWC mechanical oscillator modelling. The optimal damping at resonance approaches the radiation damping value, but is also strongly influenced by other system parameters. The third peak observed in the maximum power plot is non-resonant. It is due to the broader spectrum power capture achievable with larger power take-off damping. Active control of the power take-off damping therefore has the potential to broaden the power take-off frequency range and hence enhance the non-resonant performance of the OWC WEC device in a spectrally distributed wave environment. The physical limitation of such a control system is of course the turbine operating range.

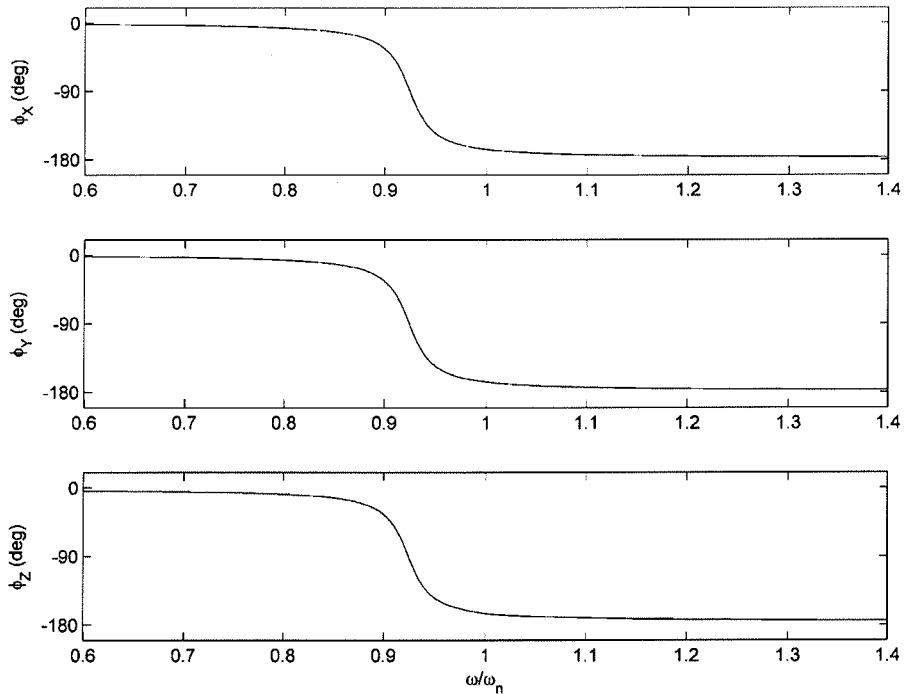


Figure 11 Floating OWC X , Y and Z motion phase at $\Omega_{os}=1$; $r=0.9$, $\zeta_s=0.01$, $\zeta_o=0.01$, $\kappa_s=0.01$, $\kappa_o=0.1$.

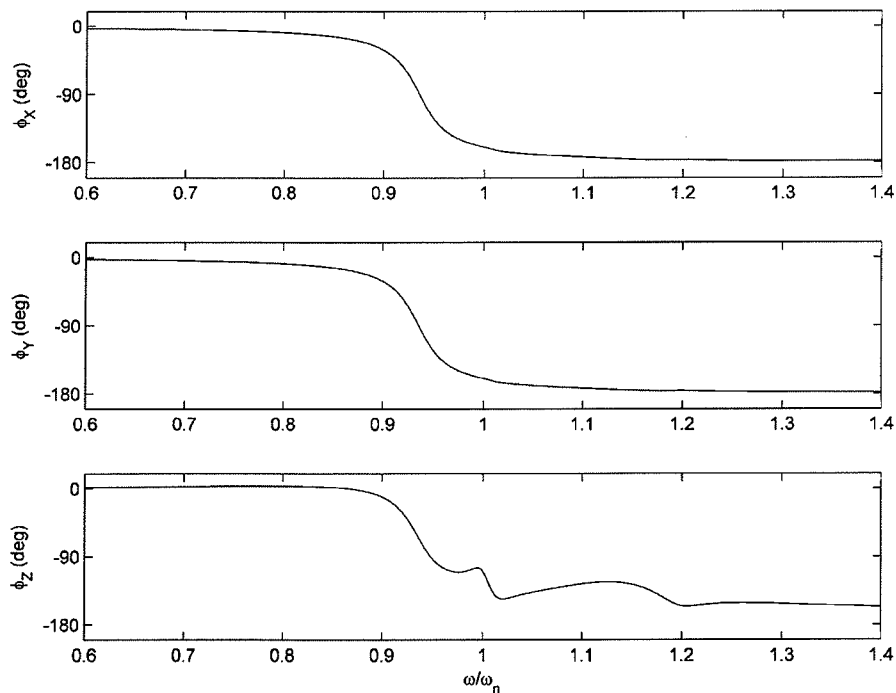


Figure 12 Floating OWC X , Y and Z motion phase at $\Omega_{os}=1.2$; $r=0.9$, $\zeta_s=0.01$, $\zeta_o=0.01$, $\kappa_s=0.01$, $\kappa_o=0.1$.

For optimal power capture, at the desired condition for air flow rate (i.e. maximal base area of OWC relative to the floating structure base area), the separation of the natural frequencies should be such that the floating structure has the lower natural frequency (i.e. $\Omega_{os} < 1$).

This is also desirable considering that oscillating water columns typically have natural frequencies higher than the incident waves (Folley & Whittaker 2005). With $\Omega_{os} < 1$, improved alignment of the system resonant response with the available wave power should result.

Air compressibility appears to have little influence on the dynamic response and power capture of a typical full scale floating OWC (i.e. κ_s and κ_r of the order 0.01 to 0.1). Essentially no phase difference is induced by the inclusion of air compressibility in the model. The natural frequencies of the structure under typical full scale conditions also vary little due to air compressibility. This should be expected since the air compressibility stiffness is at least an order of magnitude larger than the water plane stiffness of either the OWC or the floating structure.

If the OWC and structure natural frequencies coincide, power capture is very low. Under these conditions, the water column and floating structure are essentially moving in phase. Separation of the natural frequencies results in significant increases in maximum power

capture. This can be achieved through for example changes in the mooring line pre-tension (i.e. effectively changing the mass of the floating structure) and the mooring line stiffness. These methods (i.e. increasing mooring line stiffness and pre-tension) increase rather than decrease the floating structure natural frequency. Measures such as the adoption of heave plates (i.e. increasing the added mass and damping) and floating structure geometry to minimise the structure water plane area relative to the structure base area result in the more desirable frequency separation (i.e. $\Omega_{os} < 1$).

5. ACKNOWLEDGEMENTS

This work was conducted under an ARC Linkage grant (LP0776644) in conjunction with industry partner Oceanlinx Ltd.

6. REFERENCES

- Boake, C., Whittaker, T., Folley, M. & Ellen, H., (2002), 'Overview and Initial Operational Experience of the LIMPET Wave Energy Plant', Kitakyushu, Japan, International Society of Offshore and Polar Engineers.
- Brito-Melo, A., F. Neuman & Sarmiento, A., (2008), 'Full-scale data assessment in OWC Pico plant', *International Journal of Offshore and Polar Engineering*, Vol 18, No. 1, pp 27-34.
- Chudley, J., Mrina F., Ming Y. & Johnson, F., (2002), 'A tethered multiple oscillating water column wave energy device - From concept to deployment', Oslo, Norway, American Society of Mechanical Engineers.
- Falnes, J. & McIver, P., (1985), 'Wave interaction with oscillating bodies and water columns', *Hydrodynamics of Ocean Wave Energy Utilization*, Lisbon, Portugal, pp 407-418.
- Folley, M. & Whittaker, T., (2005), 'The effect of plenum chamber volume and air turbine hysteresis on the optimal performance of oscillating water columns', *Proceedings of 24th International Conference on Offshore Mechanics and Arctic Engineering (OMAE2005)*, Halkidiki, Greece.
- Gray, A., (2007), 'Oceanlinx to ride waves on Aim', *London Financial Times*, October 27.
- Mei, C. C. (1976), 'Power Extraction from Waves', *Journal of Ship Research*, Vol. 20, No. 2, pp. 63-66.
- Morris-Thomas, M. & Irvin, R. (2007), 'An investigation into the hydrodynamic efficiency of an oscillating water column', *Journal of Offshore Mechanics and Arctic Engineering*, Vol. 129, No. 4, pp. 273-278.
- Sykes, R., Lewis, A. & Thomas, G. (2009), 'A hydrodynamic study of a floating OWC', *Proceedings of the 8th European Wave and Tidal Energy Conference*, Uppsala, Sweden.
- Szumko, S., (1989), 'Mechanical Model for Oscillating Water Column with Compressibility', *Journal of Engineering Mechanics*, Vol. 115, No. 9, pp 1851-1865.
- Thiruvenkatasamy, K., Neelamani, S. and Sato, M., (1998), 'On the hydrodynamic parametric comparisons of MOWC wave energy caissons in array', *Eighth International Offshore and Polar Engineering Conference*, Montreal, Canada, pp 119-126.

* Title and name of the corresponding author: Dr. Brad Stappenbelt
Postal address: Northfields Ave, Wollongong, NSW, 2522, Australia
Telephone (incl. country code): (+61 2) 4221 8188
Fax (optional): (+61 2) 4221 3101
E-mail: brads@uow.edu.au